

See discussions, stats, and author profiles for this publication at: <https://www.researchgate.net/publication/21852076>

# Functional interactions of ligand cofactors with Escherichia coli transcription factor rho. I. Binding of ATP

ARTICLE *in* PROTEIN SCIENCE · JULY 1992

Impact Factor: 2.85 · DOI: 10.1002/pro.5560010703 · Source: PubMed

---

CITATIONS

42

---

READS

24

## 2 AUTHORS:



[Hans Geiselmann](#)

University Joseph Fourier - Grenoble 1

78 PUBLICATIONS 2,578 CITATIONS

[SEE PROFILE](#)



[Peter H. von Hippel](#)

University of Oregon

260 PUBLICATIONS 21,767 CITATIONS

[SEE PROFILE](#)

# Functional interactions of ligand cofactors with *Escherichia coli* transcription termination factor rho.

## I. Binding of ATP

JOHANNES GEISELMANN<sup>1</sup> AND PETER H. VON HIPPEL

Institute of Molecular Biology and Department of Chemistry, University of Oregon, Eugene, Oregon 97403

(RECEIVED December 27, 1991; REVISED MANUSCRIPT RECEIVED March 3, 1992)

### Abstract

*Escherichia coli* transcription termination factor rho is an RNA-dependent ATPase, and ATPase activity is required for all its functions. We have characterized the binding of ATP to the physiologically relevant hexameric association state of rho in the absence of RNA and have shown that there are six ATP binding sites per rho hexamer. This stoichiometry has been verified by a number of different techniques, including ultracentrifugation, ultrafiltration, and fluorescence titration studies. We have also shown that ATP can bind to isolated monomers of rho when the hexamer is dissociated with the mild denaturant myristyltrimethylammonium bromide, demonstrating that each protomer of rho carries an ATP binding site. The six binding sites that we observe in the rho hexamer are not equivalent; the hexamer contains three strong ( $K_d \approx 3 \times 10^6 \text{ M}^{-1}$ ) and three weak ( $K_d \approx 10^5 \text{ M}^{-1}$ ) binding sites for ATP. The binding constant of the weak binding sites is just the reciprocal of the enzymatic  $K_m$  for ATP as a substrate; thus these weak sites, as well as the strong sites, can, in principle, take part in the catalytic cycle. The asymmetry induced (or manifested) by ATP binding reduces the symmetry of the rho hexamer from a  $D_3$  to a pseudo- $D_3$  state. This "breakage" of symmetry has implications for the molecular mechanism of rho, because an asymmetric structure can lead to directional helicase activity by invoking directionally distinct RNA binding and release reactions (see Geiselmann, J., Yager, T.D., & von Hippel, P.H., 1992c, *Protein Sci.* 1, 861–873).

**Keywords:** ATP binding; *Escherichia coli*; rho; stoichiometry; symmetry; termination; transcription

Rho protein of *Escherichia coli* is required for termination of transcription by RNA polymerase and for the release of the nascent transcript at specific rho-dependent termination sites. The 47 kD protomers of rho associate to a hexamer with  $D_3$  symmetry to form the functionally active and physiologically relevant form of this protein (Finger & Richardson, 1982; Geiselmann et al., 1992a,b). Rho (in the absence of RNA polymerase) can operate as a  $5' \rightarrow 3'$  RNA–DNA helicase on appropriate substrates (Brennan et al., 1987, 1990). All the functions of rho involve the hydrolysis of nucleoside triphosphates; ATP is assumed to be the natural substrate and rho is therefore considered an ATPase.

The ATPase activity of rho is absolutely dependent on

the presence of an RNA cofactor. The highest level of ATPase activity is observed when rho is bound to a homopolymer of cytosine. In order to develop a molecular model of rho function in transcription termination, it is important to understand its interactions with its ATP substrate and RNA cofactors. The RNA binding properties of rho have been investigated in a number of laboratories (Lowery & Richardson, 1977b; Galluppi & Richardson, 1980; von Hippel et al., 1987) and are further characterized in the companion paper (Geiselmann et al., 1992c).

The interactions of rho with ATP have been examined at the functional (Lowery & Richardson, 1977a,b; Galluppi & Richardson, 1980; Stitt & Webb, 1986; Stitt, 1988) and the structural level (Engel & Richardson, 1984; Bear et al., 1985; Dombroski & Platt, 1988; Dombroski et al., 1988a,b). These studies have shown that rho possesses a distinct ATP binding domain on each protomer (Dombroski et al., 1988a,b), but that only three protomers per hexamer appear to bind a molecule of ATP

Reprint requests to: Peter H. von Hippel, Institute of Molecular Biology and Department of Chemistry, University of Oregon, Eugene, Oregon 97403.

<sup>1</sup> Present address: Département de Biologie Moléculaire, Université de Genève, 30, Quai Ernest-Ansermet, CH-1211 Genève 4, Switzerland.

(Dombroski et al., 1988b; Stitt, 1988). The ATP binding domain of rho can be separated from a distinct RNA binding domain by proteolytic cleavage (Engel & Richardson, 1984; Bear et al., 1985; Platt et al., 1989; Dolan et al., 1990). Binding and hydrolysis of ATP causes conformational changes in rho that are coupled to other conformational changes induced by RNA binding (Galluppi & Richardson, 1980; Engel & Richardson, 1984; Bear et al., 1985; Stitt, 1988). The hydrolysis of ATP proceeds via a direct transfer of the  $\gamma$ -phosphate group to water without the formation of a covalent phosphorylated enzyme or phosphorylated RNA intermediate (Stitt & Webb, 1986). The mechanism of the coupling between the ATPase activity of rho and its function as a directional RNA-DNA helicase (Brennan et al., 1987) in transcription termination remains unclear.

In this paper we extend the work of Stitt (1988) on the ATP binding properties of rho in the absence of RNA. At high concentrations of ATP we detect an additional three ATP binding sites per rho hexamer. This result is confirmed by several independent determinations of the ATP binding stoichiometry, using different techniques. We have previously shown (Geiselmann et al., 1992b) that the rho hexamer is the functionally important association state of rho and that the hexamer is composed of a trimer of dimers characterized by  $D_3$  symmetry (Seifried et al., 1991; Geiselmann et al., 1992a). The existence of two classes of ATP binding sites corroborates this trimer of dimers organization and also demonstrates that each dimer does not possess an exact twofold symmetry axis (as required for a structure characterized by  $D_3$  symmetry). One protomer of each rho dimer binds ATP more tightly than does the other. As a consequence we now consider the overall symmetry of the rho hexamer to be of the pseudo- $D_3$  type.

This finding has important implications for possible molecular mechanisms of rho in transcription termination and as an RNA-DNA helicase. In order to achieve a directional helicase activity (Brennan et al., 1987, 1990) using elementary RNA binding and release reactions one has to invoke an asymmetric structure. Binding of the RNA ligand further reduces the symmetry of the (now) pseudo- $D_3$  symmetrical hexamer (Geiselmann et al., 1992c). The resulting structure provides the basis for a proposed physical model for the function of rho protein in transcription termination (Geiselmann et al., in prep.).

## Results

The parameters that characterize the interaction of a ligand with a macromolecule are the binding stoichiometry and the binding constant. If the macromolecule possesses several classes of binding sites, one must both determine the total number of binding sites for the ligand and characterize the binding affinities of each class of sites.

### Titration with $\epsilon$ -ATP

In order to determine the stoichiometry of ATP binding to the rho hexamer we have made use of the fact that the fluorescence of the ATP analogue, 1, $N^6$ -etheno-adenosine 5'-triphosphate ( $\epsilon$ -ATP), is efficiently quenched by acrylamide. When  $\epsilon$ -ATP is bound to rho it is (at least partially) removed from the solvent environment and thus is no longer as accessible to this nonionic quencher of fluorescence. Binding of  $\epsilon$ -ATP to rho in the presence of acrylamide therefore leads to an increase in the apparent fluorescence of this moiety compared to that of free  $\epsilon$ -ATP. The observed fluorescence change on binding is about sevenfold and is readily measurable.

We have confirmed that  $\epsilon$ -ATP can serve as a substrate for rho ATPase, and that  $V_{max}$  for this moiety is comparable to that obtained with ATP. Furthermore we have verified that the concentration of acrylamide used in these experiments does not affect the ATPase activity of rho. A typical titration curve obtained by this technique is shown in Figure 1A.

In order to reach a binding plateau in these experiments we have used relatively high concentrations of rho. At such protein concentrations it is difficult to detect binding heterogeneity (see the Discussion), permitting us to fit the data to a simple binding isotherm (Equation 1). Nonlinear least-squares fits to these data yield stoichiometries between 0.93 and 1.04  $\epsilon$ -ATP molecules bound per rho protomer and an apparent binding constant for  $\epsilon$ -ATP to rho ranging (in different experiments) from  $3 \times 10^5 \text{ M}^{-1}$  to  $6 \times 10^5 \text{ M}^{-1}$ .

In a graphical representation (Fig. 1A) the stoichiometry of binding corresponds to the intersection of the tangent to the initial part of the binding curve with the plateau value of the fluorescence (the graphical method is exact if  $Pn \gg 1/K$ , see Equation 1). The use of a high rho concentration in these experiments assures a reliable determination of the stoichiometry; a nearly linear initial portion of the binding curve and a clear titration end point (binding plateau) are seen Figure 1A.

The uncertainty in this determination of  $\epsilon$ -ATP binding stoichiometry (indicated as 95% confidence intervals in the legend to Fig. 1) is comparable to pipetting and other measurement errors (i.e., a few percent). A reliable value of this parameter is expected because the titration is essentially stoichiometric (the rho concentration used is about eightfold higher than the reciprocal of the apparent binding constant). We therefore conclude from these experiments that one molecule of  $\epsilon$ -ATP is bound per protomer of rho.

Figure 1B shows that  $\epsilon$ -ATP binds to the same sites on rho as does ATP, as these substrates bind competitively. After each titration of rho with  $\epsilon$ -ATP we were able to displace all of the  $\epsilon$ -ATP by back titration with ATP (Fig. 1B). At the point at which one-half of the originally bound  $\epsilon$ -ATP is replaced by ATP (i.e., the fluorescence

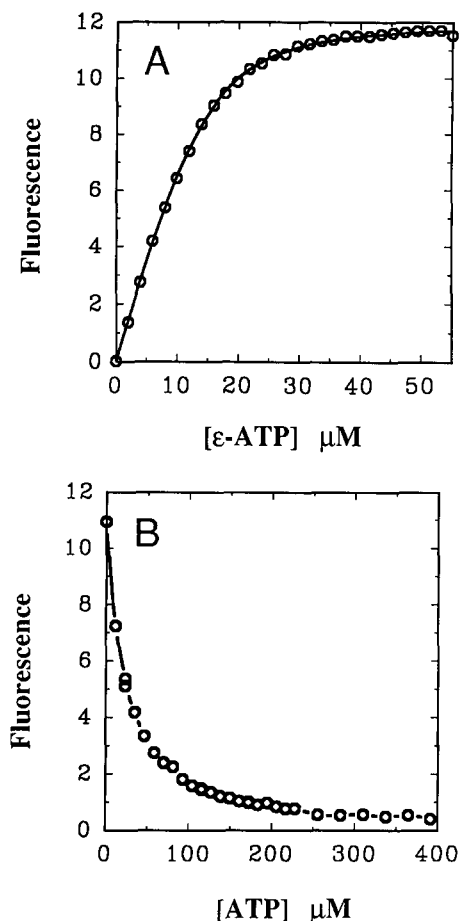


**Fig. 1.** Titration of rho with  $\epsilon$ -ATP. **A:** The fluorescence (in arbitrary units; corrected for the background of free  $\epsilon$ -ATP and for the volume change upon ligand addition) is plotted as a function of the concentration of  $\epsilon$ -ATP. The concentration of rho was 16.5  $\mu$ M (in protomers). The data were fit to a simple binding isotherm (Equation 1) with parameters:  $K = 5.6 \times 10^5 \text{ M}^{-1}$  (95% confidence limits:  $4.8 \times 10^5 \text{ M}^{-1}$  and  $6.6 \times 10^5 \text{ M}^{-1}$ ),  $n = 0.94$  (95% confidence limits: 0.90 and 0.97). **B:** Back titration of the titration shown in A with ATP. All of the  $\epsilon$ -ATP is competed off with ATP. At the point of half-maximal fluorescence the ratio of free  $\epsilon$ -ATP to free ATP is about 3:1.

change has dropped to one-half its maximal value), the ratio of the concentrations of free  $\epsilon$ -ATP to free ATP is about 3:1. We therefore estimate that the apparent binding constant for ATP to rho at these elevated protein concentrations is  $\sim 1.5 \times 10^6 \text{ M}^{-1}$ . As indicated above, the binding constant for ATP obtained by this means is only an apparent constant because these experiments cannot exclude the existence of several classes of binding sites. If ATP binds with different affinities to the six protomers within a hexamer this apparent binding constant will represent an intermediate value between the strongest and weakest microscopic constants. We emphasize that the existence of two classes of ATP binding sites (as suggested by other binding experiments described below) is not con-

tradicted by these fluorescence studies at high protein concentration.

Fluorescence titrations (versus total ligand concentration) performed at rho concentrations of 2  $\mu$ M do not reach a plateau, even with 10  $\mu$ M added  $\epsilon$ -ATP. This observation is consistent with binding site heterogeneity of  $\epsilon$ -ATP binding and argues for the existence of a low affinity ( $K < 5 \times 10^5 \text{ M}^{-1}$ ) class of binding sites for at least some of the  $\epsilon$ -ATP ligands. Because titrations at low rho concentrations do not show a clear end point (one of the adjustable parameters in the curve-fitting routine) they have not been used for stoichiometry or binding constant determinations.

We repeated the titration of rho with  $\epsilon$ -ATP under the conditions described above, but in the presence of a saturating concentration of (dC)<sub>10</sub>. The apparent binding constant for  $\epsilon$ -ATP is three- to fourfold weaker than that observed in the absence of the (dC)<sub>10</sub> ligand, suggesting some allosteric coupling between the ATP and the oligonucleotide binding sites of rho (see Geiselmann et al., 1992c). The reliability of the fit involved in determining stoichiometry is reduced, due to the lower apparent binding constant, but the best fit remains the same: i.e., one  $\epsilon$ -ATP is bound per rho protomer.

#### Semidenaturing gel experiments

To further confirm the critical point that each protomer of rho possesses an ATP binding site, we repeated the experiment (described in Geiselmann et al., 1992a) of separating different association states of rho on a semidenaturing gel. In this particular experiment we included ATP with the rho sample. A stoichiometry of three ATPs bound per rho hexamer could, for example, reflect the existence of ATP binding sites formed at the interface between individual subunits. However, in this model one would not expect to see ATP bound to rho monomers. Comparison of the autoradiograph and the silver-stained gel shows that ATP does bind to rho monomers in this experiment (Fig. 2). We know that ATP is not carried along nonspecifically by the detergent because ATP does not comigrate with any of the marker proteins. In addition, no ATP binding was observed when the gel was run in a phosphate (Geiselmann et al., 1992a) or Tris-borate-EDTA buffer (Hammes & Rickwood, 1981). (Phosphate is a competitive inhibitor of ATP binding and EDTA would complex the  $\text{Mg}^{2+}$  that is required for ATP binding [Stitt, 1988].)

The binding of ATP to rho monomers that we observe in this experiment thus appears to be specific; this observation strengthens our earlier conclusion that each individual rho protomer carries one ATP binding site (see Geiselmann et al., 1992a). Binding is not stoichiometric under the gel conditions used, and it is therefore impossible to estimate a binding constant for ATP to the rho

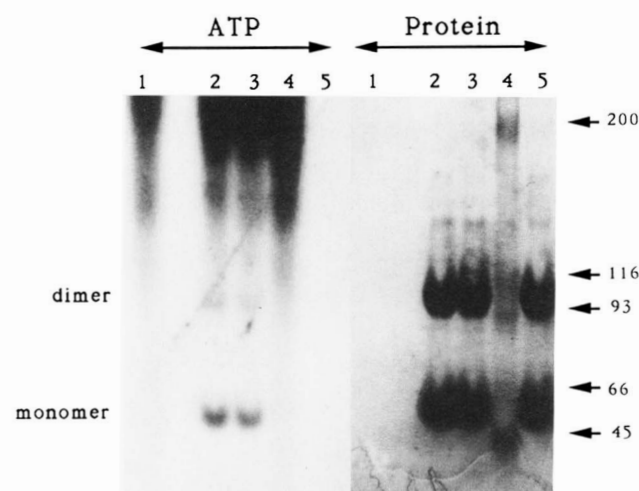


**Fig. 2.** Rho protein run on a semidenaturing gel in the presence of  $\gamma$ -labeled  $^{32}\text{P}$ -ATP. The silver-stained gel is shown on the right and the corresponding autoradiograph on the left. Lane 1, 25  $\mu\text{M}$  ATP; lane 2, 20  $\mu\text{M}$  rho and 25  $\mu\text{M}$  ATP; lane 3, 20  $\mu\text{M}$  rho and 6  $\mu\text{M}$  ATP; lane 4, molecular weight markers and 25  $\mu\text{M}$  ATP; lane 5, 20  $\mu\text{M}$  rho. The molecular weights of the marker proteins are indicated on the right side of the gel. The positions of the rho monomer and dimer are shown on the left side of the gel. The smear of ATP at the top of the gel is present even in the lane that does not contain any protein; the presence of ATP does not perturb the dimerization (compare the lanes with and without ATP).

monomer from these data (in addition the presence of the detergent provides a different solvent environment than the normal aqueous surround). Nevertheless, it should be noted that more ATP is bound to the monomer than to the dimer, even though roughly the same amount (by mass) of protein is present in both bands.

### ATP binding measurements

The following experiments examine in more detail the binding affinity of ATP for rho. The quantities that must be measured in determining the binding constant for a ligand-macromolecule interaction are the concentrations of free and bound ligand. The total concentration of macromolecule is determined simply by measuring the amount used in the reaction. In general one also knows the total amount of input ligand. Thus, the only parameter that must be determined experimentally is the concentration of free ligand after equilibrium has been attained; the concentration of bound ligand is calculated from conservation of mass. We have used a variety of methods to measure ATP binding to rho in order to cancel out any systematic errors that may characterize a particular technique.

The experiments described above have shown that the

rho hexamer can bind a total of six molecules of ATP. The following experiments are consistent with this stoichiometry, but we have not attempted to derive an independent measure of the binding stoichiometry from these measurements (see Materials and methods) in order to reduce the number of independent variables that must be fit and thus to increase the accuracy of the binding constants obtained. Thus, in what follows, we focus on binding constant determinations and assume a binding stoichiometry of six molecules of ATP per rho hexamer.

### Preparative ultracentrifugation

We have measured ATP binding to rho by centrifugation in a Beckman Airfuge. This technique is based on the fact that free ATP does not sediment appreciably in the centrifugal field used, whereas protein-bound ATP does. By taking advantage of this difference in sedimentation behavior we can separate free from bound ATP (Howlett et al., 1978). Binding equilibrium is maintained at all times during the sedimentation process. We determined the concentration of ATP by including trace amounts of  $\gamma$ -labeled  $^{32}\text{P}$ -ATP, thus relating the concentration of ATP to the radioactivity measured by scintillation counting. The radioactive ATP stocks that we used in these experiments typically contained a radioactive contaminant that did not bind to rho protein (the concentration of the contaminant is the same in the top and bottom fractions after the centrifuge run). We have compensated for the presence of these impurities by analyzing for ATP using thin-layer chromatography (TLC) and quantitated the autoradiographs obtained by densitometry with a Biomed Instruments Model SL-504-XL scanning densitometer. The data points obtained by this Airfuge technique are included in Figures 3 and 4 as diamonds.

### Analytical ultracentrifugation

The same principle of separation of free and bound ATP was exploited in experiments using the model E analytical ultracentrifuge. Free ATP does not sediment, and its concentration is determined directly by measuring the band of constant absorbance remaining at the top of the centrifuge cell. The concentration of bound ATP is calculated by conservation of mass, and this value is confirmed experimentally by measuring the absorbance of the sedimenting material containing rho and bound ATP. The data from two such experiments carried out at high concentrations of rho (squares in Figs. 3, 4) show a saturation of rho with more than one ATP bound per dimer of rho and thus confirm the stoichiometry of one ATP bound per rho monomer. The sedimentation coefficient (10.2S) is identical for samples with or without added ATP, proving that ATP binding does not change the hexameric association state of rho under the experimental conditions used.

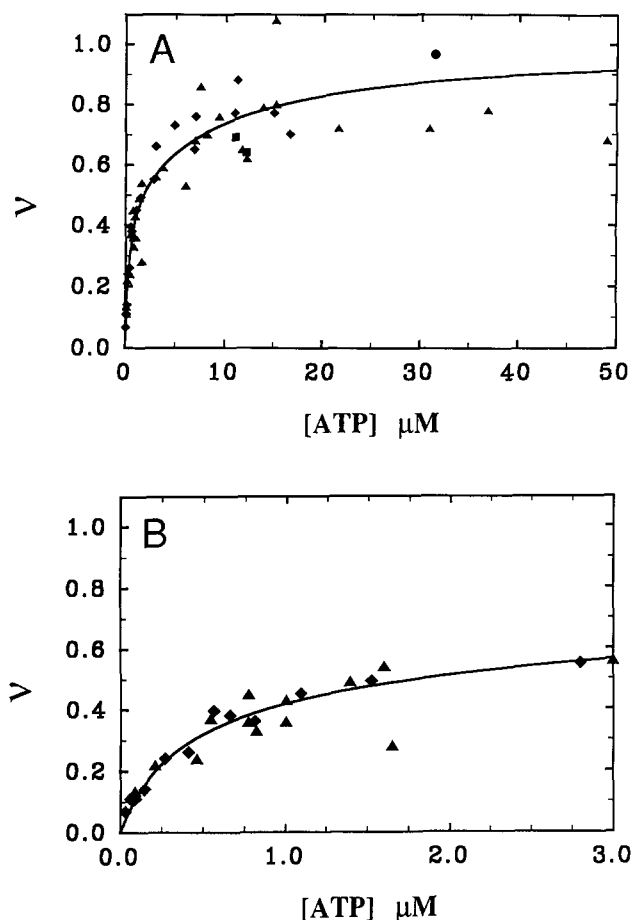


**Fig. 3.** Direct plot of the ATP binding data. The triangles are data obtained with the ultrafiltration technique, the diamonds represent Air-fuge experiments, and the squares are data from sedimentation in the Model E analytical ultracentrifuge. **A:** Data over the full concentration range of ATP. **B:** Enlarged view of the low concentration data. The biphasic behavior of the curve is clearly visible as an apparent saturation value at 0.5 moles of ligand bound per mole of rho monomer.

#### Ultrafiltration

In this technique mixtures of rho and ATP are passed through a filter that is impermeable to the protein. The filter used has a molecular weight cutoff of 30 kDa. Free ATP easily passes through the filter and is collected in the bottom of the cell. The concentration of free ATP does not change during the filtration process, even though the concentration of rho increases in the compartment above the filter. Very good data have already been obtained by this technique by Stitt (1988) using  $\sim 1 \mu\text{M}$  concentrations of rho (concentrations are in units of rho protomers). Data obtained at high rho (and high ATP) concentrations address the determination of the binding constants to the weak binding sites and the limiting value of the overall binding stoichiometry. The large majority of data points obtained by this ultrafiltration technique (triangles in Figs. 3, 4) were determined by a direct spectrophotomet-

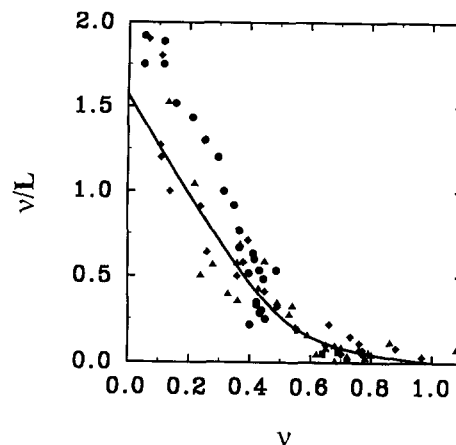


**Fig. 4.** Scatchard plot of the ATP binding data. The line is the best fit to the combined data using a preexistent asymmetry model (see text). The binding constants are:  $K_1 = 3 \times 10^6 \text{ M}^{-1}$  (95% confidence limits:  $1.9 \times 10^6 \text{ M}^{-1}$  and  $5.4 \times 10^6 \text{ M}^{-1}$ ),  $K_2 = 0.09 \times 10^6 \text{ M}^{-1}$  (95% confidence limits:  $0.06 \times 10^6 \text{ M}^{-1}$  and  $0.15 \times 10^6 \text{ M}^{-1}$ ). The data from Stitt (1988) are included for comparison (circles). The other symbols are as in Figure 1.

ric measurement of the concentration of free ATP and did not involve radioactively labeled ATP.

#### Summary of ATP binding data

The ATP binding data obtained by all these methods, presented in Figure 3 in the form of a direct binding isotherm and in Figure 4 as a Scatchard plot, clearly show that the binding stoichiometry of ATP to rho is greater than three ATPs per rho hexamer and that it is most likely that there are six ATPs bound per hexamer.

It is also clear that the Scatchard plot is nonlinear. This indicates that the rho hexamer contains more than one class of ATP binding sites as defined by binding affinity. This fact is more clearly brought out in the enlarged, low concentration part of the binding curve shown in Figure 3B. The high affinity binding sites have become saturated at  $\sim 3 \mu\text{M}$  ATP. The circles included in the Scatchard plot of Figure 4 are taken from Stitt (1988) and show the agreement of the binding measurements in this concentration range. The best-fit curve does not include these data points and passes below the circles, reflecting the slight difference in binding constant obtained by the two laboratories. We note that this difference in binding constants ( $4.3 \times 10^6 \text{ M}^{-1}$  versus  $3.0 \times 10^6 \text{ M}^{-1}$ ) might reflect the different solvent conditions used in the two studies: i.e., 50 mM KCl and 1 mM  $\text{MgCl}_2$  versus 100 mM KCl and 10 mM  $\text{MgCl}_2$ .

#### Curve fitting

The combined data were fit to Equation 2, as described in the Materials and methods. The binding model used

assumes two classes of ATP binding sites, with one weak and one strong site per rho dimer. The best fit is obtained with a strong binding constant ( $K_1$ ) of  $3.0 \times 10^6 \text{ M}^{-1}$  and a weak binding constant ( $K_2$ ) of  $0.09 \times 10^6 \text{ M}^{-1}$ . (The 95% confidence intervals of the data fit for  $K_1$  are  $1.9 \times 10^6 \text{ M}^{-1}$  and  $5.4 \times 10^6 \text{ M}^{-1}$ , and for  $K_2$  are  $0.06 \times 10^6 \text{ M}^{-1}$  and  $0.15 \times 10^6 \text{ M}^{-1}$ .) Even though the binding data show some scatter, the values of the two binding constants are significantly different and a model involving only a single binding constant can be excluded. The fitting routine processes the unmanipulated data, i.e., the binding saturation of the protein ( $\nu$ ) as a function of ATP concentration added (Fig. 3). This presentation is then transformed to the Scatchard form (Fig. 4) for easier visualization of the binding classes. The exact numerical values obtained depend, of course, on the particular model used in the data analysis (see the Discussion).

## Discussion

We have characterized the binding of ATP to rho in the absence of RNA, because under these conditions the RNA-dependent ATPase of this protein is not activated. The interaction of rho with its other cofactor, RNA, is addressed in the accompanying paper (Geiselmann et al., 1992c). Binding and hydrolysis of ATP is required for all functions of the rho protein. The characterization of these ligand binding interactions therefore has important implications for molecular mechanisms of rho action. The parameters of interest are the stoichiometries and binding constants of ATP to rho.

We have shown that rho is a hexamer under physiological protein and salt concentrations (Gogol et al., 1991; Seifried et al., 1991; Geiselmann et al., 1992b). The experiments we describe here to measure ATP binding were performed under conditions that favor the association of rho protomers to the hexameric state. At low concentrations of rho, ATP can drive association toward the hexamer (Finger & Richardson, 1982), and binding measurements at these concentrations may be complicated by such coupled equilibria. At the high rho concentrations used here these considerations are not relevant. We have verified this important point experimentally in our binding measurements using the model E ultracentrifuge. The measured sedimentation coefficient is 10.2S in the absence as well as in the presence of ATP. Thus rho remains hexameric in our experiments.

Because the rho hexamer is characterized by  $D_3$  symmetry (Geiselmann et al., 1992a), it is reasonable to assume a binding stoichiometry for ATP of either three or six molecules per hexamer. A stoichiometry of three molecules per hexamer has been measured by Stitt (1988) at low concentrations of rho. Such a stoichiometry could reflect the presence of ATP binding sites formed jointly by two rho protomers at a subunit interface. Genetic evidence argues against this; Platt and coworkers (Dom-

broski & Platt, 1988) have found that a part of the amino acid sequence of rho is homologous to known ATP binding sites and have confirmed this identification by site-directed mutagenesis and affinity labeling experiments (Dombroski et al., 1988a,b). Thus, each rho protomer should carry a potential ATP binding site. Physical biochemical arguments presented in Seifried et al. (1991) and Geiselmann et al. (1992a) also support this conclusion.

The experiments presented in this paper address the following issues: (1) the limiting stoichiometry of ATP binding (i.e., are all six potential ATP binding sites per hexamer used?); and (2) the binding constant(s) of ATP to these sites. The conclusions drawn from the different experiments are summarized in Table 1. To simplify the analysis we have not entertained stoichiometries that are not reasonably related to the known structure of the rho oligomer (i.e., we do not expect to find five ATP molecules bound per rho hexamer).

## ATP binding site stoichiometry

The stoichiometry of ATP binding has been specifically addressed by fluorescence titration and semidenaturing gel experiments. The fluorescent ATP analogue,  $\epsilon$ -ATP, was used to monitor binding spectroscopically. In such experiments one can only measure the total concentration of macromolecule and ligand. We have therefore used a simple binding isotherm (Equation 1) to model the binding and have obtained a very good fit of the  $\epsilon$ -ATP binding data to this equation. The algebraic solution of the binding equation with site heterogeneity is rather complicated and is not practical for use in curve-fitting routines.

In the fitting procedure we varied three parameters: the stoichiometry ( $n$ ), the association constant ( $K_a$ ), and the scale parameter ( $C$ ) that relates the fluorescence signal to binding saturation. The multiple possibilities of param-

**Table 1.** Summary of ATP binding data

Experimental method	Conclusions <sup>a</sup>
Sedimentation in airfuge	$K_1 = 3.0$ [1.8, 4.6]; $K_2 = 0.14$ [0.09, 0.21]
Ultrafiltration	$K_1 = 2.8$ [1.1, 9.0]; $K_2 = 0.09$ [0.04, 0.19]
Analytical ultracentrifugation	$n > 0.5$ ; rho remains hexameric
Combination of above	$K_1 = 3.0$ [1.9, 5.4]; $K_2 = 0.09$ [0.06, 0.151]
Fluorescence titration	$n = 1.0$ ; $K_{app} = 1.5$
Semidenaturing gel studies	One ATP binding site per rho monomer

<sup>a</sup> All binding constants are in units of  $10^6 \text{ M}^{-1}$ . Numbers in brackets indicate the 95% confidence intervals of the fit (see Materials and methods).

eter adjustment allow binding to two classes of binding sites to be well fit by Equation 1 under certain conditions. The use of simulated data sets with Equation 1 shows that a 10-fold difference in binding constants for two classes of binding sites can easily be masked, provided that the protein concentration is high enough to make binding to the weak sites almost stoichiometric. In this case the fitting program cannot distinguish whether the first part of the binding curve actually corresponds to tight or to very tight binding, as both exhibit a linear increase in binding signal at the low end of the curve. As a consequence, possible biphasicity in the binding isotherm cannot be detected at the high concentrations of macromolecule used in these experiments. A curve fit with Equation 1 under these conditions leads to a stoichiometry slightly lower than the sum of all binding sites and to an intermediate apparent binding constant.

The  $\epsilon$ -ATP titrations have therefore been useful for determining limiting stoichiometry but are unable to distinguish between different classes of binding sites. Fluorescence titrations at a high concentration of rho yield a stoichiometry of one molecule of  $\epsilon$ -ATP bound per rho protomer. We therefore conclude that the hexamer possesses six  $\epsilon$ -ATP binding sites. Back titration with ATP displaces all of the bound  $\epsilon$ -ATP and demonstrates that the two ligands bind competitively to the same sites.

The existence of an ATP binding site on each rho monomer has been confirmed by an experiment in which rho is dissociated into monomers and dimers by a mild denaturant myristyltrimethylammonium bromide (MTAB). Rho, like many proteins (see Akin et al., 1985), conserves at least part of its functional structure under these conditions. The denaturant binds to the protein and confers a constant charge upon it. Therefore one can separate the different associated species on such a gel on a basis very analogous to that underlying the commonly used SDS gel electrophoresis procedure. The gel shown in Figure 2 demonstrates that ATP can bind to monomers of rho. This finding confirms the limiting binding stoichiometry of one ATP per rho monomer and also argues against an ATP binding site formed at a subunit interface.

The binding of ATP to rho had been independently characterized by Stitt (1988) at low rho (1  $\mu$ M) and ATP (0.05–2.5  $\mu$ M) concentrations. From these data Stitt concluded that rho carries only three ATP binding sites per hexamer. Binding data that we have collected using a number of techniques agrees very well with the results of Stitt obtained at low concentrations of ATP and rho; her data points (included in Fig. 3A as circles) superimpose on ours. However, in binding studies performed at higher concentrations of ATP and rho we detect additional ATP binding sites. Even though it is not possible to determine the precise stoichiometry of ATP binding solely on the basis of these data, it is clear from Figures 3 and 4 that there are more than three ATP binding sites per hexamer. This finding, coupled with information on the structure

of rho, makes it most reasonable to assume that the limiting stoichiometry is indeed six molecules of ATP bound per rho hexamer. This value has therefore been assumed in the model-dependent curve-fitting procedures (Equation 2) that we have used to determine binding constants.

### *Heterogeneity of ATP binding site affinities*

The Scatchard plot presented in Figure 4 is curved, suggesting the existence of at least two classes of ATP binding sites differing in binding affinity. Attempts to fit the data with a single binding constant lead to highly correlated residuals and definitively rules out this model. We have fit the data with a nonlinear least-squares procedure, using a binding model with six ATP binding sites per hexamer divided into two classes containing three strong and three weak sites, respectively. Other models for ATP binding (like three classes of ATP binding sites, etc.) were not considered on the grounds of parsimony and the known structure and symmetry of the rho hexamer (Gogol et al., 1991; Geiselmann et al., 1992a,b).

Even though there is some scatter in the binding data, the confidence intervals of the binding constants clearly indicate a very pronounced difference in ATP affinity for the two classes of sites. The fit yields a binding constant of about  $3 \times 10^6 \text{ M}^{-1}$  for the strong sites (agreeing well with the value of  $4.3 \times 10^6 \text{ M}^{-1}$  measured by Stitt [1988]). The weak sites display a 20–30-fold lower affinity for ATP ( $K \sim 10^5 \text{ M}^{-1}$ ). This value is just the reciprocal of the  $K_m$  of rho for ATP, which means that these sites could also be involved in the catalytic process.

The numerical values obtained for the binding constant depend, of course, on the model used to fit the data. We have considered two models to describe the binding of ATP to rho. Both models assume that two ATP molecules (with different affinities) are bound per functional dimer (see Seifried et al., 1991; Geiselmann et al., 1992a). The asymmetry within a dimer with respect to ATP binding can preexist, or it can be induced by the binding of the first ATP to the dimer (Galley et al., 1988). The algebraic form of the binding equations differs only by the numerical values of the binding constants. If the preexistent asymmetry model is described by the binding constants  $K_1$  and  $K_2$ , then the alternative model of induced asymmetry will be described by the binding constants  $K_1'$  and  $K_2'$ , where  $K_1' = (K_1 + K_2)/2$ , and  $K_2' = 2K_1'K_2'/(K_1 + K_2)$ . The binding constants reported above were derived assuming a preexistent asymmetry model. In the alternative model the stronger binding constant would be decreased by roughly a factor of two, and the weaker binding constant would be increased by about the same factor. The quality of the fit remains the same for both models.

The semidenaturing gel experiments run in the presence of ATP (Fig. 2) are consistent with the existence of two classes of ATP binding sites per rho dimer. Whereas most



of the protein in the gel is in the form of dimers, more ATP is bound to the monomeric form. This observation is consistent with a model in which the affinity of a rho protomer for ATP is modulated (weakened) by intersubunit interactions with an adjacent protomer.

The allosteric alteration of the ATP binding site upon dimerization could also affect the interaction of this site with the detergent. It is therefore not possible to describe the precise nature of the allosteric interaction or to calculate interaction energies based on this experiment. In particular, we cannot distinguish between a ligand-induced and a preexisting asymmetry for ATP binding within the rho dimer.

### *Conclusions and implications*

In Seifried et al. (1991) and Geiselmann et al. (1992a) we showed that rho protein associates as a trimer of dimers. The data presented here lend support to the view that the functional unit of rho is a dimer, as it is the smallest repeating unit of the hexamer. The subunits within this dimer are not equivalent, because they bind ATP with differing affinities. The functional asymmetry within the dimer could preexist in the unligated rho hexamer, or it could be induced by ATP binding.

It is known from several studies that ATP binding causes a conformational change of the protein, rendering it less susceptible to proteolytic digestion by trypsin (Engel & Richardson, 1984; Bear et al., 1985). This conformational change is coupled to conformational changes induced by RNA binding (Stitt, 1988). ATP binding may also lead to a stabilization of intersubunit contacts between rho monomers. This is manifested at low rho concentrations as a conversion of rho to a higher average association state in the presence of ATP (Finger & Richardson, 1982) and is a clear indication that ATP binding perturbs intersubunit contacts. It is possible that the conformational changes caused by the binding of ATP to one rho subunit of a dimer are communicated to the adjacent subunit, resulting in a decrease in the binding affinity for ATP of the second subunit.

The breakage of exact  $D_3$  symmetry has important implications for the molecular mechanism of rho action. An interesting and important property of rho is the directionality of the helicase activity. A completely symmetric structure cannot exhibit directionality by simple association and dissociation reactions. Of course, molecular "levers and pullies" could produce directionality, but such structures would presumably require very complex molecular designs. Furthermore, if each subunit were equipped with such complicated mechanisms it would seem unnecessary for rho to exist in a specific oligomeric association state. The breakage of symmetry introduced by (or manifested by) ATP binding is the first step toward the establishment of a unique function for each subunit within the hexamer. The number of equivalent entities

has been reduced from six to three. The binding of the other functional cofactor of rho, i.e., RNA, could reduce this number still further (see Geiselmann et al., 1992c).

The ATP molecules bound in the strong ATP binding sites can be hydrolyzed in the presence of RNA (Stitt et al., 1988). The existence of the weaker ATP binding sites suggests that the nonequivalent subunits within a dimer could alternately assume one or the other state. In the second half of a reaction cycle the weakly bound ATP molecules would become strongly bound by a conformational change within the dimer. In this case ATP permanently fixed to one-half of the dimer might be expected to block the reaction cycle and considerably inhibit ATPase activity. Dombroski et al. (1988b) have covalently attached a nonhydrolyzable ATP analogue to three protomers within a rho hexamer and indeed have observed almost complete inhibition of the ATPase activity. We propose that the functional unit of rho is the dimer (see also Richardson & Ruteshouser, 1986; Stitt, 1988; Seifried et al., in prep.). This dimer is asymmetric with respect to ATP binding and can undergo a conformational transition that converts the high affinity site into the low affinity site and vice versa. A complete reaction cycle of rho would then involve (at least) two such conformational changes in series, after which the original state is restored. We will show elsewhere (Geiselmann et al., in prep.) how this conformational change can be coupled to RNA binding and lead to a physical model of rho action of the sort that we believe might be involved in transcription termination.

### **Materials and methods**

#### *Reagents and buffers*

The standard binding buffer in all ATP binding experiments contained 100 mM KCl, 10 mM  $MgCl_2$ , 40 mM Tris-HCl (pH 7.8), and 0.1 mM EDTA. In some reactions we included 5% glycerol and/or 0.1 mM dithiothreitol (DTT). The presence or absence of glycerol or DTT did not change any of our results. ATP was purchased from PL-Biochemicals and contained less than 1% contaminating ADP.  $\gamma$ -Labeled  $^{32}P$ -ATP was purchased from New England Nuclear and had a specific activity of 111 TBq/mmol. It contained up to 30% of a radioactive contaminant (determined by TLC on a PEI-cellulose plate developed with a running buffer of 0.3 M  $KH_2PO_4$ , pH 7.0). The fluorescent ATP analogue,  $\epsilon$ -ATP, was purchased from Pharmacia. It contained about 5% of ADP (or  $\epsilon$ -ADP) but was found to be free of other contaminants using the above TLC assay. Rho protein was prepared as described in Geiselmann et al. (1992b). The concentration of rho was determined spectrophotometrically using an absorbance of 3.25 OD at 280 nm for a 10-mg/mL solution (Geiselmann et al., 1992b), after correction for light scattering. Concentrations of rho are pre-

sented in units of rho protomers, based on a protomer molecular weight of 46,974 Da.

#### *Airfuge method for measuring binding*

Small samples of protein can be sedimented in an Airfuge manufactured by the Spinco Division of Beckman Instruments. We have followed essentially the procedure described by Howlett et al. (1978). A small aluminum rotor (diameter ~4 cm) is suspended and accelerated by jets of compressed air. The cylindrical sample tubes are set at an angle of 18° from the axis of rotation. At the maximum operating speed of 100,000 rpm the centrifugal field at the bottom of the tube is about  $160,000 \times g$ . Rho protein sediments to the bottom of the tubes in less than 1 h under these experimental conditions.

All experiments were carried out at room temperature. We loaded 100  $\mu$ L of a mixture of rho and ATP (containing trace amounts of radioactively labeled ATP). The concentration of rho in these experiments was typically 6  $\mu$ M, but ranged from 1  $\mu$ M to 15  $\mu$ M in particular experiments. The concentration of ATP was varied from 0.1  $\mu$ M to 30  $\mu$ M. We typically included 1.5 pmol of radioactive ATP in a 100- $\mu$ L binding reaction. This corresponds to a concentration of radioactive ATP of about 15 nM and a specific activity of about 1,000 dpm (disintegrations per minute) per microliter of binding reaction.

After the centrifuge run we withdrew the top 40  $\mu$ L of the sample and analyzed for ATP by scintillation counting and for rho by ATPase activity. The duration of the centrifuge run was adjusted so that about 1% of the rho remained in the upper fraction (typically 1 h). We also analyzed the lower fraction after stirring to assure conservation of mass. We estimated the amount of contaminating radioactivity in the ATP by densitometry of autoradiographs of samples run on a PEI-cellulose TLC plate with a 0.3 M  $\text{KH}_2\text{PO}_4$  (pH 7.0) running buffer. The concentration of free ATP was determined from the radioactivity in the top portion of the sample (corrected for radioactive contaminants in the ATP). The concentration of bound ATP was calculated on the basis of the total rho and ATP concentrations used in the experiment.

#### *Ultrafiltration*

A mixture of rho and ATP in standard binding buffer was loaded onto a Centricon 30 microconcentrator (Amicon Corp.) and centrifuged in an SS-34 rotor at room temperature at 5,000 rpm for about 5 min. Sample volumes were between 0.3 and 0.5 mL. The concentration of rho protomers varied from 1  $\mu$ M to 30  $\mu$ M, and the concentration of ATP ranged between 0.1  $\mu$ M and 80  $\mu$ M. The concentration of free ATP was determined by scintillation counting or by direct spectrophotometric analysis of the filtrate. The amount of contaminating radioactivity was used as a correction factor, as in the Airfuge

method. The ultrafiltration procedure, except for the concentrations chosen, is the same as that used by Stitt (1988).

#### *Analytical ultracentrifugation of rho and ATP*

Mixtures of rho and ATP (in binding buffer) were sedimented in a model E analytical ultracentrifuge cell as described in Geiselmann et al. (1992b). Instead of analyzing the boundary by standard methods we measured only the height of the plateaus of the sedimenting species (rho and rho-ATP complex) and of the nonsedimenting species (free ATP). Fixing the slit of the UV detection optics at a particular position in the cell (e.g., within the free ATP region), we could vary the wavelength to obtain a crude spectrum of the sample. In this way we determined the concentration of free and bound ATP spectrophotometrically within the analytical ultracentrifuge cell.

#### *Fluorescence titration*

Fluorescence titrations of rho with  $\epsilon$ -ATP were performed using an SLM Smart 8000 spectrofluorometer linked to an HP-87 microcomputer for data storage and control of the automatic titrator. The excitation wavelength was 320 nm (the excitation maximum of  $\epsilon$ -ATP), and emission was monitored at 400 nm (the emission maximum); the slit width was set at 4 nm on both monochromators. The concentration of rho protomers was typically between 10  $\mu$ M and 30  $\mu$ M. In addition to the components of the regular binding buffer, we included 200 mM acrylamide in these experiments. The acrylamide quenches the fluorescence of free  $\epsilon$ -ATP, but not that of bound  $\epsilon$ -ATP. Fluorescent  $\epsilon$ -ATP was added, using a computer-controlled autotitrator, into a stirred 3-mL fluorescence cuvette (thermostated at 25 °C) containing the 1,500- $\mu$ L sample. The titrant was contained in 34-gauge Teflon tubing at a concentration of ~3 mM. After each titration the  $\epsilon$ -ATP was competed away from the rho protein by back titration with ATP. A blank titration containing no rho protein under the identical conditions was paired with each experiment. A straight line was fitted to the blank and subtracted from the titration data and from the data for the competition titration with ATP. The resulting titration curves were then analyzed as described below and in the Results.

#### *Curve fitting*

The fluorescence titrations of rho with  $\epsilon$ -ATP were modelled using the following binding equation (simple binding isotherm):

$$\text{Signal} = C\{Pn + L + 1/K - [(Pn + L + 1/K)^2 - 4PnL]^{1/2}\}/2, \quad (1)$$

where  $P$  is the total concentration of macromolecule (rho),  $L$  is the total ligand concentration ( $\epsilon$ -ATP),  $K$  is the binding constant,  $n$  is the number of binding sites per macromolecule (number of ATP binding sites per rho monomer), and  $C$  is the scale parameter that relates the binding signal to the binding saturation. Equation 1 describes the interaction between a ligand and a macromolecule with  $n$  independent and equivalent binding sites.

The other techniques were used to measure ATP binding directly in terms of binding saturation as a function of the concentration of free ligand. We find two classes of ATP binding sites (see Results), and binding was therefore modeled with the following equation (Galley et al., 1988):

$$\nu = \frac{K_1[A] + K_2[A] + 2K_1K_2[A]^2}{2(1 + K_1[A] + K_2[A] + K_1K_2[A]^2)}, \quad (2)$$

where the binding saturation,  $\nu$  (expressed as the number of molecules of ATP bound per rho monomer), is a function of the concentration of free ATP,  $[A]$ .  $K_1$  and  $K_2$  are the binding constants to the two classes of ATP binding sites.

Data fitting was done with the program OPDATA (P. Bennett and C.J. Kost, Triumph Software, 4004 Westbrook Mall, Vancouver, British Columbia V6T 2A3, Canada) running on a VAX computer and with Pascal programs taken from Press et al. (1989). The programs employ nonlinear least-squares fitting routines for parameter optimization.

The quality of the curve fits was assessed essentially as described in the Appendix of McSwiggen et al. (1988). The best fit is described by the set of parameters that minimizes the sum of the squared deviations ( $S$ ),  $S_{min}$ . One parameter at a time is varied away from its optimal value while optimizing the remaining parameters to maintain the lowest possible sum of squared deviations. In this way one always remains in the lowest "valley" of the contour map, as shown in the Appendix of McSwiggen et al. (1988).

The amount by which the sum of the squared deviations ( $S$ ) increases as a parameter is moved away from its optimal value is a measure of the probability that the true value of the parameter lies between these bounds. For a data set containing  $N$  points, to be fitted by a function with  $m$  adjustable parameters, there is a probability,  $p$ , that the true value of a parameter lies between the best fit value (where  $S = S_{min}$ ) and the value of the parameter where  $S = S_p$  if (Press et al., 1989):

$$S_p = S_{min}(1 + \chi_m^2/\chi_{N-m}^2). \quad (3)$$

The calculation of this limit rests on the assumption that the errors in the measurement are normally distributed. The quotient of the chi-squared distributions ( $\chi_m^2/\chi_{N-m}^2$ ) with  $m$  and  $N - m$  degrees of freedom, re-

spectively, can be calculated using the  $F$ -distribution,  $F(m, N - m)$ , at the probability level  $p$ . For an implementation of a Pascal program see Press et al. (1989). We report here the 95% confidence intervals of the data fits.

### Semidenaturing gels

Gel electrophoresis of a mixture of rho and ATP on a semidenaturing gel was performed as described in Geiselman et al. (1992a), with the following modifications. Instead of phosphate buffer, a 50 mM KCl, 5 mM MgCl<sub>2</sub>, and 40 mM Tris-HCl (pH 8.0) buffer was used in the gel and in the reservoirs. Rho protein was loaded into the wells in this buffer at a concentration of about 20  $\mu$ M rho monomer. We also added ATP (and trace amounts of radioactive  $\gamma$ -labeled <sup>32</sup>P-ATP) into the loading buffer to a concentration between 6 and 100  $\mu$ M; the detergent MTAB was present at a concentration of 0.2% (w/v). After electrophoresis the gel was frozen at  $-70^\circ\text{C}$  and exposed to X-ray film. The gel was silver-stained on the following day as described in Hammes and Rickwood (1981).

### Acknowledgments

This work has been submitted (by J.G.) to the Graduate School of the University of Oregon in partial fulfillment of the requirements for the Ph.D. degree in Chemistry. These studies were supported in part by USPHS research grants GM-15792 and GM-29158 (to P.H.v.H.) and by a grant from the Lucille P. Markey Charitable Trust. P.H.v.H. is an American Cancer Society Research Professor of Chemistry. We are very grateful to Dr. Steven Seifried for helpful discussions of binding analysis procedures.

### References

- Akin, D.T., Shapira, R., & Kincade, J.M., Jr. (1985). The determination of molecular weights of biologically active proteins by cetyltrimethylammonium bromide-polyacrylamide gel electrophoresis. *Anal. Biochem.* 145, 170-176.
- Bear, D.G., Andrews, C.L., Singer, J.D., Morgan, W.D., Grant, R.A., von Hippel, P.H., & Platt, T. (1985). *Escherichia coli* transcription termination factor rho has a two-domain structure in its activated form. *Proc. Natl. Acad. Sci. USA* 82, 1911-1915.
- Brennan, C.A., Dombroski, A.J., & Platt, T. (1987). Transcription termination factor rho is an RNA-DNA helicase. *Cell* 48, 945-952.
- Brennan, C.A., Steinmetz, E.J., Spear, P., & Platt, T. (1990). Specificity and efficiency of rho-factor helicase activity depends on magnesium concentration and energy coupling to NTP hydrolysis. *J. Biol. Chem.* 265, 5440-5447.
- Dolan, J.W., Marshall, N.F., & Richardson, J.P. (1990). Transcription termination factor rho has three distinct domains. *J. Biol. Chem.* 265, 5747-5754.
- Dombroski, A.J., Brennan, C.A., Spear, P., & Platt, T. (1988a). Site-directed alterations in the ATP-binding domain of rho protein affects its activities as a termination factor. *J. Biol. Chem.* 263, 18802-18809.
- Dombroski, A.J., LaDine, J.R., Cross, R.L., & Platt, T. (1988b). The ATP-binding site on rho protein. *J. Biol. Chem.* 263, 18810-18815.
- Dombroski, A.J. & Platt, T. (1988). Structure of rho factor: An RNA-binding domain and a separate region with strong similarity to

- proven ATP-binding domains. *Proc. Natl. Acad. Sci. USA* 85, 2538-2542.
- Engel, D. & Richardson, J.P. (1984). Conformational alterations of transcription termination protein rho induced by ATP and by RNA. *Nucleic Acids Res.* 12, 7389-7400.
- Finger, L.R. & Richardson, J.P. (1982). Stabilization of the hexameric form of *Escherichia coli* protein rho under ATP hydrolysis conditions. *J. Mol. Biol.* 156, 203-219.
- Galley, W.C., Bouvier, M., Clas, S.D., Brown, G.R., & St.-Pierre, L.E. (1988). A simplified analysis of Scatchard plots for systems with two interacting binding sites. *Biopolymers* 27, 79-86.
- Galluppi, G.R. & Richardson, J.P. (1980). ATP-induced changes in the binding of RNA synthesis termination protein rho to RNA. *J. Mol. Biol.* 138, 513-539.
- Geiselmann, J., Seifried, S.E., Yager, T.D., Liang, C., & von Hippel, P.H. (1992a). Physical properties of the *E. coli* transcription termination factor rho. II. Quaternary structure of the rho hexamer. *Biochemistry* 31, 121-132.
- Geiselmann, J., Yager, T.D., Gill, S.C., Calmettes, P., & von Hippel, P.H. (1992b). Physical properties of the *E. coli* transcription termination factor rho. I. Association states and geometry of the rho hexamer. *Biochemistry* 31, 111-121.
- Geiselmann, J., Yager, T.D., & von Hippel, P.H. (1992c). Functional interaction of ligand cofactors with *Escherichia coli* transcription termination factor rho. II. Binding of RNA. *Protein Sci.* 1, 861-873.
- Gogol, E.P., Seifried, S.E., & von Hippel, P.H. (1991). Structure and assembly of the *Escherichia coli* transcription termination factor rho and its interactions with RNA. I. Cryoelectron microscopic studies. *J. Mol. Biol.* 221, 1127-1138.
- Hammes, B.D. & Rickwood, D. (1981). *Gel Electrophoresis of Proteins*. IRL Press, Oxford, Washington, D.C.
- Howlett, G.J., Yeh, E., & Schachman, H.K. (1978). Protein<sup>®</sup> ligand binding studies with a table-top, air-driven, high-speed centrifuge. *Arch. Biochem. Biophys.* 190, 809-819.
- Lowery, C. & Richardson, J.P. (1977a). Characterization of the nucleoside triphosphate phosphorylase (ATPase) activity of RNA synthesis termination factor rho. Enzymatic properties and effects of inhibitors. *J. Biol. Chem.* 252, 1375-1380.
- Lowery, C. & Richardson, J.P. (1977b). Characterization of the nucleoside triphosphate phosphorylase (ATPase) activity of RNA synthesis termination factor rho. Influence of synthetic RNA homopolymers and random copolymers of the reaction. *J. Biol. Chem.* 252, 1381-1385.
- McSwiggen, J.A., Bear, D.G., & von Hippel, P.H. (1988). Interactions of *Escherichia coli* transcription termination factor rho with RNA. I. Binding stoichiometries and free energies. *J. Mol. Biol.* 199, 609-622.
- Platt, T., Brennan, C.A., Dombroski, A.J., & Spear, P. (1989). *Molecular Biology of RNA*. A.R. Liss, New York, pp. 325-334.
- Press, W.H., Flannery, B.P., Teukolsky, S.A., & Vetterling, W.T. (1989). *Numerical Recipes in Pascal*, Chapter 14. Cambridge University Press, Cambridge, UK.
- Richardson, J.P. & Ruteshouser, C.E. (1986). Rho factor-dependent transcription termination. Interference by a mutant rho. *J. Mol. Biol.* 189, 413-419.
- Seifried, S.E., Bjornson, K.P., & von Hippel, P.H. (1991). Structure and assembly of the *Escherichia coli* transcription termination factor rho and its interactions with RNA. II. Physical chemical studies. *J. Mol. Biol.* 221, 1139-1151.
- Stitt, B.L. (1988). *Escherichia coli* transcription termination protein rho has three hydrolytic sites for ATP. *J. Biol. Chem.* 263, 11130-11137.
- Stitt, B.L. & Webb, M.R. (1986). Absence of a phosphorylated intermediate during ATP hydrolysis by *Escherichia coli* transcription termination protein rho. *J. Biol. Chem.* 261, 15906-15909.
- von Hippel, P.H., Yager, T.D., Bear, D.G., McSwiggen, J.A., Geiselmann, J., Gill, S.C., Linn, J.D., & Morgan, W.D. (1987). Mechanistic aspects of transcript elongation and rho-dependent termination in *Escherichia coli*. In *RNA Polymerase and the Regulation of Transcription* (Reznikoff, W.S., Burgess, R.R., Dahlberg, J.E., Gross, C.A., Record, M.T., Jr., & Wickens, M.P., Eds.), pp. 325-334. Elsevier, New York.